Journal of Chromatography A, 1218 (2011) 5166–5174

Contents lists available at ScienceDirect

Journal of Chromatography A

journal homepage: www.elsevier.com/locate/chroma

A theoretical plate model accounting for slow kinetics in chromatographic elution

J.J. Baeza-Baeza*, M.C. García-Álvarez-Coque

Departament de Química Analítica, Universitat de València, c/Dr. Moliner 50, 46100 Burjassot, Spain

ARTICLE INFO

Article history:
Received 28 March 2011
Received in revised form 20 May 2011
Accepted 23 May 2011
Available online 30 May 2011

Keywords:
Liquid chromatography
Peak profile
Slow mass transfer
Plate models
Martin and Synge model
Extended model

ABSTRACT

The chromatographic elution has been studied from different perspectives. However, in spite of the simplicity and evident deficiencies of the plate model proposed by Martin and Synge, it has served as a basis for the characterization of columns up-to-date. This approach envisions the chromatographic column as an arbitrary number of theoretical plates, each of them consisting of identical repeating portions of mobile phase and stationary phase. Solutes partition between both phases, reaching the equilibrium. Mobile phase transference between the theoretical plates is assumed to be infinitesimally stepwise (or continuous), giving rise to the mixing of the solutions in adjacent plates. This yields an additional peak broadening, which is added to the dispersion associated to the equilibrium conditions. It is commonly assumed that when the solute concentration is sufficiently small, chromatographic elution is carried out under linear conditions, which is the case in almost all analytical applications. When the solute concentration increases above a value where the stationary phase approximates saturation (i.e. becomes overloaded), non-linear elution is obtained. In addition to overloading, another source of non-linearity can be a slow mass transfer. An extended Martin and Synge model is here proposed to include slow mass-transfer kinetics (with respect to flow rate) between the mobile phase and stationary phase. We show that there is a linear relationship between the variance and the ratio of the kinetic constants for the mass transfer in the flow direction (τ) and the mass transfer between the mobile phase and stationary phase (ν), which has been called the kinetic ratio ($\kappa = \tau/\nu$). The proposed model was validated with data obtained according to an approach that simulates the solute migration through the theoretical plates. An experimental approach to measure the deviation from the equilibrium conditions using the experimental peak variances and retention times at several flow rates is also proposed.

1. Introduction

Finding an accurate model to describe the chromatographic elution is practically an unsolvable problem, as has been commented by Giddings and Eyring [1], due to the complexity and the unknown factors involved in the process, beginning with the nature of the multi-site surface up to the particularities of the stationary phase packing. In spite of this, a huge effort has been done to develop models to understand the peak shape and the main factors that affect it [2–7].

The models that describe the equilibrium conditions in liquid chromatography can be classified as linear and non-linear [6,8]. In the linear models, the amount of solute associated to the stationary phase is assumed to be proportional to its concentration in the mobile phase. This implies that the equilibrium between the mobile phase and stationary phase is instantaneous. Also, the sample components do not compete for the stationary phase, nor interact among them; their elution is, therefore, independent from each other. This means that each peak in a mixture has independent characteristics and is identical to that obtained upon elution of an isolated standard.

Linear chromatography has been studied from three different perspectives: (i) the plate models proposed by Martin and Synge [9], and Craig [10], (ii) the differential rate model that describes the mass balance and mass-transfer kinetics, proposed by Lapidus and Amundson [11], and van Deemter et al. [12], and extensively applied by other authors [13–17], and (iii) the statistical models developed by Giddings and Eyring [1], and followed by Dondi et al. [18,19].

The plate models envision the chromatographic column as an arbitrary number of theoretical plates, each of them consisting of identical repeating portions of stationary phase and mobile phase. It is assumed that the solute partitions between both phases, reaching the equilibrium. In the model proposed by Craig [10], there is no mixing mechanism and the mobile phase is transferred downstream completely from one plate to the following, in a discrete way (stepwise). The final band broadening is produced exclusively by the quantitativeness of the distribution equilibrium of the solute

* Corresponding author. Tel.: +34 96 354 3184; fax: +34 96 354 4436.
E-mail address: Juan.Baeza@uv.es (J.J. Baeza-Baeza).

0021-9673/$ – see front matter © 2011 Elsevier B.V. All rights reserved.
doi:10.1016/j.chroma.2011.05.086

between the two phases along the column theoretical plates, which gives rise to solute dispersion along the theoretical plates. The Craig model gives rise to a distribution, which can be approximated to a Gaussian profile with the following variance [4]:

$$\sigma^2 = \frac{t_R(t_R - t_0)}{N} \quad (1)$$

where t_R is the retention time (time at the peak maximum), t_0 the dead time (the time at which a non-retained solute elutes) and N the number of theoretical plates (or efficiency). According to this model, a non-retained solute (i.e. in the absence of interactions) would elute with the dead volume, with a null peak width.

In the model proposed by Martin and Synge [9], mobile phase transference between plates is assumed to be infinitesimally stepwise (or continuous), giving rise to the mixing of the solutions in adjacent plates. This yields an additional peak broadening, which is added to the dispersion associated to the equilibrium conditions. The final peak profile is an Erlang distribution [20], which can also be approximated to a Gaussian with a variance:

$$\sigma^2 = \frac{t_R^2}{N} \quad (2)$$

In the absence of interactions between solute and stationary phase (i.e. for a non-retained solute), this model predicts a minimal peak broadening:

$$\sigma_0^2 = \frac{t_0^2}{N} \quad (3)$$

In spite of the simplicity and evident deficiencies of the Martin and Synge plate model, it has served as a basis for the characterization of columns up-to-date. These deficiencies have been partially overcome by newer models [4,7,17]. We make a new proposal, which is explained below.

It is commonly assumed that when the solute concentration is sufficiently small, chromatographic elution is carried out under linear conditions, which is the case in almost all analytical applications. When the solute concentration increases above a value where the stationary phase approximates saturation (i.e. becomes overloaded), non-linear elution conditions are obtained. This means that the concentration in the stationary phase increases slower than in the mobile phase. Accordingly, solutes at different concentrations tend to move along the column at different velocities: the peaks become asymmetrical and the retention times depend on the solute concentration in the mobile phase. This behaviour is described by non-linear isotherms that follow different models, as the Langmuir or Freundlich-type isotherms [8].

In addition to overloading, another source of non-linearity can be a slow mass transfer. In this case, the changes in the solute concentration in the stationary phase will depend, not only on the solute concentration in the mobile phase, but also on the stationary phase. In this work, the Martin and Synge model is extended to include slow mass-transfer kinetics between the mobile phase and stationary phase.

2. Theory

The plate count theory assumes that the chromatographic column is divided in N theoretical plates. According to this, we have developed a global approach that considers the partition process along the whole column. A system of N differential equations (one equation for each theoretical plate) is obtained, which is solved using the Laplace transform. The approach is applied below to equilibrium and slow mass-transfer conditions in chromatography.

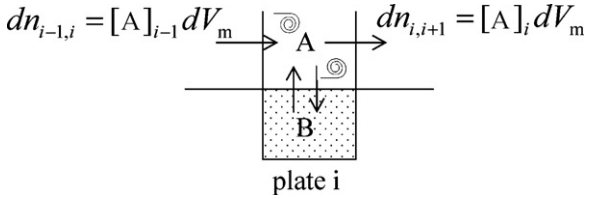

Fig. 1. Change in the moles of solute in the mobile phase associated to a theoretical plate. A and B indicate the solute in the mobile phase and stationary phase, respectively; $dn_{i-1,i}$ and $dn_{i,i+1}$ denote the moles that enter and leave the i theoretical plate in dt.

2.1. Linear equilibrium elution

2.1.1. Peak function

Fig. 1 depicts the mass transfer for a given solute associated to an i theoretical plate, in an infinitesimal time interval dt. The change in the moles of solute in a theoretical plate will be:

$$dn_i = [A]_{i-1} dV_m - [A]_i dV_m \quad (4)$$

where $[A]_i$ and $[A]_{i-1}$ are the solute concentrations in the mobile phase associated to the i and $i-1$ theoretical plates, respectively, and dV_m is the mobile phase volume that is transferred from one plate to the next in the time interval dt. Assuming that the distribution equilibrium between mobile phase and stationary phase is reached instantaneously, the partition constant is expressed as:

$$K = \frac{[B]_i}{[A]_i} = \frac{b_i}{a_i}\frac{V_m}{V_s} \quad (5)$$

$[B]_i$ is the solute concentration in the stationary phase, and V_m and V_s are the volumes of mobile phase and stationary phase associated to a theoretical plate, respectively, which do not change along the column; a_i and b_i are the moles of solute in the mobile phase and stationary phase in the i theoretical plate, respectively. The total moles in the i theoretical plate will be:

$$n_i = a_i + b_i \quad (6)$$

From Eq. (5):

$$n_i = a_i + K a_i \frac{V_s}{V_m} = a_i\left(1 + K\frac{V_s}{V_m}\right) \quad (7)$$

The moles of solute in the mobile phase can be thus expressed as a fraction of the total moles:

$$a_i = p n_i \quad (8)$$

with

$$p = \frac{1}{\left(1 + K\frac{V_s}{V_m}\right)} = \frac{1}{1+k} = \frac{t_0}{t_R} \quad (9)$$

k being the retention factor:

$$k = \frac{t_R - t_0}{t_0} \quad (10)$$

Therefore, the solute concentration in the mobile phase associated to the i theoretical plate will be:

$$[A]_i = \frac{p n_i}{V_m} \quad (11)$$

On the other hand, dV_m and dt are related through:

$$dV_m = u dt = \frac{N V_m}{t_0} dt \quad (12)$$

where u is the flow rate and NV_m represents the total column volume accessible to the mobile phase. Going back to Eq. (4), and taking into account Eqs. (11) and (12):

$$dn_i = \frac{N}{t_0} p n_{i-1} dt - \frac{N}{t_0} p n_i dt \quad (13)$$

The change in the moles of solute in the time interval dt will be:

$$\frac{dn_i}{dt} = \tau p n_{i-1} - \tau p n_i \tag{14}$$

where τ is the flow rate expressed as the number of theoretical plates per time unit:

$$\tau = \frac{N}{t_0} \tag{15}$$

Based on Eq. (14), a system of differential equations can be written to describe the change in the moles of solute in the mobile phase associated to each theoretical plate, considering the whole column:

$$\begin{aligned} n_1^{(1)} &= -\tau p n_1 \\ n_2^{(1)} &= \tau p n_1 - \tau p n_2 \\ &\vdots \\ n_N^{(1)} &= \tau p n_{N-1} - \tau p n_N \end{aligned} \tag{16}$$

where $n_i^{(1)} = dn_i/dt$, and $n_1 \ldots n_N$ are the moles of solute in each theoretical plate, which change with time. Eqs. (16) can be solved by applying a Laplace transform, which reduces a linear differential equation with constant coefficients to an algebraic equation [21]:

$$n_i^{(1)} = r n_i - n_{i,0} \tag{17}$$

In Eq. (17), r is the Laplace variable in the r-domain, and $n_{i,0}$ the moles of solute in the i theoretical plate at $t = 0$. The number of moles at $t = 0$ is n_0 for the first theoretical plate, and zero for the other plates. Therefore:

$$\begin{aligned} -n_0 &= -(r + \tau p) n_1 \\ 0 &= \tau p n_1 - (r + \tau p) n_2 \\ &\vdots \\ 0 &= \tau p n_{N-1} - (r + \tau p) n_N \end{aligned} \tag{18}$$

The first equation can be solved independently:

$$n_1 = \frac{n_0}{(r + \tau p)} \tag{19}$$

Once n_1 is known, n_2 can be calculated as:

$$n_2 = n_0 \frac{\tau p}{(r + \tau p)^2} \tag{20}$$

and so on for the next theoretical plates up to the last one:

$$n_N = n_0 \frac{(\tau p)^{N-1}}{(r + \tau p)^N} \tag{21}$$

The solute monitored at the detector is the portion that flows out of the N plate in each dt. The peak profile at the detector will be described by:

$$f(r) = \tau p n_N = n_0 \left(\frac{\tau p}{r + \tau p} \right)^N \tag{22}$$

The integration of this equation in the time-domain between zero and ∞ yields n_0, since the whole amount of analyte that enters into the column and migrates through it, must flow out. The normalized peak function in the r-domain is:

$$f_n(r) = \left(\frac{\tau p}{r + \tau p} \right)^N = (F_r)^N \tag{23}$$

Considering the inverse Laplace transform [21]:

$$\frac{1}{(r + \tau p)^N} = \frac{t^{N-1}}{(N-1)!} e^{-\tau p t} \tag{24}$$

the function in the time domain will be:

$$f(t) = \frac{(\tau p)^N}{(N-1)!} t^{N-1} e^{-\tau p t} \tag{25}$$

which is equivalent to equations reported by Martin and Synge [9], and Felinger [4].

Eq. (25) is an Erlang distribution, which is related with the Gamma function [20]. It can be checked that it is a normalized equation [22]:

$$\int_0^\infty f(t)dt = \frac{(\tau p)^N}{(N-1)!} \int_0^\infty t^{N-1} e^{-\tau p t} dt = \frac{(\tau p)^N}{(N-1)!} \frac{(N-1)!}{(\tau p)^N} = 1 \tag{26}$$

2.1.2. Mean time, variance and skewness of the peak function

To obtain the moments about the origin, the following property of the Laplace transformation should be considered [13,21]:

$$\mu_k' = \int_0^\infty t^k f(t) dt = (-1)^k \lim_{r \to 0} \frac{d^k f_n(r)}{dr^k} \tag{27}$$

From Eq. (23):

$$\mu_0' = (-1)^0 (F_{r=0})^N = 1 \tag{28}$$

since $F_{r=0} = 1$. The mean value is the first moment about the origin:

$$\mu_1' = \bar{t} = (-1) N (F_{r=0})^{N-1} F_{r=0}^{(1)} \tag{29}$$

where:

$$F_{r=0}^{(1)} = \frac{-\tau p}{(r + \tau p)^2} = -\frac{1}{\tau p} \tag{30}$$

By combining Eqs. (9), (10), and (15), (23), (29) and (30):

$$\mu_1' = \bar{t} = \frac{N}{\tau p} = t_0(1 + k) = t_R \tag{31}$$

The variance is the second moment about the mean:

$$\mu_2 = \sigma^2 = \mu_2' - \mu_1'^2 \tag{32}$$

From Eqs. (23) and (27):

$$\mu_2{}' = (-1)^2 [N(N-1) F_{r=0}^{N-2} (F_{r=0}^{(1)})^2 + N F_{r=0}^{N-1} F_{r=0}^{(2)}] \tag{33}$$

and from Eq. (30):

$$F_{r=0}^{(2)} = \frac{2\tau p}{(r + \tau p)^3} = \frac{2}{(\tau p)^2} \tag{34}$$

which yields:

$$\mu_2' = \frac{N(N-1)}{(\tau p)^2} + \frac{2N}{(\tau p)^2} \tag{35}$$

From Eq. (32) (see also Eq. (31)):

$$\mu_2 = \sigma^2 = \frac{N}{(\tau p)^2} = \frac{t_R^2}{N} \tag{36}$$

The third moment about the mean is related to the peak skewness (asymmetry) [23]. It can be calculated as:

$$\mu_3 = \mu_3' - 3\mu_1'\mu_2' + 2\mu_1'^3 \tag{37}$$

Again, from Eqs. (27) and (33):

$$\begin{aligned} \mu'_3 = (-1)^3 [&N(N-1)(N-2) F_{r=0}^{N-3} (F_{r=0}^{(1)})^3 \\ &+ 3N(N-1) F_{r=0}^{N-2} F_{r=0}^{(1)} F_{r=0}^{(2)} + N F_{r=0}^{N-1} F_{r=0}^{(3)}] \end{aligned} \tag{38}$$

where:

$$F_{r=0}^{(3)} = \frac{-6\tau p}{(r + \tau p)^4} = -\frac{6}{(\tau p)^3} \tag{39}$$

and

$$\mu_3' = \frac{N(N-1)(N-2)}{(\tau p)^3} + \frac{6N(N-1)}{(\tau p)^3} + \frac{6N}{(\tau p)^3} \tag{40}$$

From Eq. (37), together with Eqs. (31), (35) and (40):

$$\mu_3 = \frac{2N}{(\tau p)^3} = \frac{2t_R^3}{N^2} \tag{41}$$

Finally, the peak skewness can be estimated from [20]:

$$\gamma_1 = \frac{\mu_3}{\mu_2^{3/2}} = \frac{2}{N^{1/2}} \tag{42}$$

Therefore, in the Martin and Synge model at equilibrium conditions, the retention time and peak width only depend on the partition constant, the flow rate and the number of theoretical plates in the column. The peak skewness decreases with N.

2.2. Slow mass transfer

2.2.1. Peak function

We will now consider that the mass-transfer rate between the mobile phase and stationary phase is finite. To understand how this affects the peak profile, we will outline an extended Martin and Synge model, which includes explicitly the mass-transfer kinetics. When the kinetics is sufficiently slow (with respect to the flow rate), the elution depends on both moles of solute in the mobile phase (a) and stationary phase (b). The mass transfer from the mobile phase to the stationary phase in each theoretical plate is described by the flow-rate equation [24]:

$$J_{A,i} = \left(\frac{\partial a_i}{\partial t}\right)_{\text{transfer}} = \nu(a_{\text{eq},i} - a_i) \tag{43}$$

where a_i are the total moles of solute in the mobile phase, $a_{\text{eq},i}$ the moles at equilibrium with the stationary phase, and ν the mass-transfer rate constant between both phases. When the equilibrium is reached, Eq. (8) holds. Taking into account Eq. (6):

$$a_{\text{eq},i} = pn_i = p(a_i + b_i) \tag{44}$$

By substituting Eq. (44) in Eq. (43) and making:

$$q = 1 - p \tag{45}$$

$$J_{A,i} = \left(\frac{\partial a_i}{\partial t}\right)_{\text{transfer}} = \nu p b_i - \nu q a_i = s b_i - m a_i \tag{46}$$

Consequently, the change in the moles of solute in the stationary phase will be:

$$J_{B,i} = -\left(\frac{\partial a_i}{\partial t}\right)_{\text{transfer}} = m a_i - s b_i \tag{47}$$

Besides the mass transfer between the mobile phase and stationary phase, there is a mobile phase flow through the theoretical plates. For two consecutive plates, and taking into account Eqs. (8) and (14):

$$\left(\frac{\partial a_i}{\partial t}\right)_{\text{flow}} = \tau a_{i-1} - \tau a_i \tag{48}$$

The change in the moles of solute due to both processes will be:

$$\frac{da_i}{dt} = s b_i - m a_i + \tau a_{i-1} - \tau a_i = \tau a_{i-1} - (\tau + m) a_i + s b_i \tag{49}$$

$$\frac{db_i}{dt} = m a_i - s b_i \tag{50}$$

For the whole column, the following system of differential equations can be outlined:

$$\begin{aligned}
a_1^{(1)} &= -(\tau + m)a_1 + s b_1 \\
b_1^{(1)} &= m a_1 - s b_1 \\
a_2^{(1)} &= \tau a_1 - (\tau + m)a_2 + s b_2 \\
b_2^{(1)} &= m a_2 - s b_2 \\
&\vdots \\
a_N^{(1)} &= \tau a_{N-1} - (\tau + m)a_N + s b_N \\
b_N^{(1)} &= m a_N - s b_N
\end{aligned} \tag{51}$$

where $a_i^{(1)} = da_i/dt$ and $b_i^{(1)} = db_i/dt$; $a_1 \ldots a_N$ and $b_1 \ldots b_N$ are the moles of solute in the mobile phase and stationary phase associated to each theoretical plate, respectively, which change with time. Solving the system of equations by applying a Laplace transform (Eq. (17)) for the variables a_i and b_i, and assuming again that n_0 are the moles of solute in the first theoretical plate, the following system of algebraic equations is obtained:

$$\begin{aligned}
-n_0 &= -(r + \tau + m)a_1 + s b_1 \\
0 &= m a_1 - (r + s) b_1 \\
0 &= \tau a_1 - (r + \tau + m)a_2 + s b_2 \\
0 &= m a_2 - (r + s) b_2 \\
&\vdots \\
0 &= \tau a_{N-1} - (r + \tau + m)a_N + s b_N \\
0 &= m a_N - (r + s) b_N
\end{aligned} \tag{52}$$

From the two first equations:

$$-n_0 = \left(-(r + \tau + m) + \frac{ms}{r + s}\right) a_1 \tag{53}$$

from which:

$$\begin{aligned}
a_1 &= n_0 \frac{r + s}{(r + \tau + m)(r + s) - ms} = n_0 \frac{r + s}{r^2 + (m + s + \tau)r + \tau s} \\
&= n_0 \frac{r + s}{(r + r_1)(r + r_2)}
\end{aligned} \tag{54}$$

Taking into account that (from Eqs. (45) and (46)):

$$m + s = \nu q + \nu p = \nu \tag{55}$$

the roots r_1 and r_2 in Eq. (54) can be calculated as:

$$r_1 = \frac{\nu + \tau - \sqrt{(\nu + \tau)^2 - 4\tau s}}{2} = \frac{S - R}{2} \tag{56}$$

$$r_2 = \frac{\nu + \tau + \sqrt{(\nu + \tau)^2 - 4\tau s}}{2} = \frac{S + R}{2} \tag{57}$$

Once a_1 is known (Eq. (54)), a_2 can be calculated, and so on for all theoretical plates. Thus, for the N theoretical plate:

$$a_N = n_0 \tau^{N-1} \left(\frac{r + s}{(r + r_1)(r + r_2)}\right)^N \tag{58}$$

Similarly to Eq. (22), the detected solute will be:

$$f(r) = \tau a_N \tag{59}$$

and the normalized function:

$$f_n(r) = \left(\frac{\tau(r + s)}{(r + r_1)(r + r_2)}\right)^N = (F_r)^N \tag{60}$$

In this case, the transformation of the function in the r-domain Eq. (60) to that in the time-domain ($f(t)$) is not direct. In Appendix A, we develop a transformed $f(t)$ function for conditions close to the equilibrium.

2.2.2. Mean time, variance and skewness of the peak function

The mean time, variance and skewness of the peak function corresponding to a slow mass-transfer (Eq. (60)) are calculated similarly to the equilibrium conditions as shown in Section 2.1.2. It should be noted that at slow mass-transfer conditions (see Eqs. (56) and (57)):

$$r_1 r_2 = \tau s \tag{61}$$

$$r_1 + r_2 = S = \nu + \tau \tag{62}$$

being $s = vp$ (see Eq. (46)). In order to calculate the mean time, variance and skewness, we need the following derivatives:

$$F_r^{(1)} = \tau \frac{(r+r_1)(r+r_2) - (r+s)(2r+r_1+r_2)}{(r+r_1)^2(r+r_2)^2}$$

$$= -\tau \frac{r^2 + 2rs - r_1 r_2 + s(r_1+r_2)}{(r+r_1)^2(r+r_2)^2} = -\tau \frac{r^2 + 2rs + s\nu}{(r+r_1)^2(r+r_2)^2} \tag{63}$$

where

$$F_{r=0}^{(1)} = -\frac{1}{\tau p} \tag{64}$$

For the second derivative:

$$F_r^{(2)} = 2\tau \frac{r^3 + 3r^2 s + 3rs\nu + s\nu^2 - \tau s^2 + \tau s\nu}{(r+r_1)^3(r+r_2)^3} \tag{65}$$

$$F_{r=0}^{(2)} = 2\frac{1+\kappa(1-p)}{(\tau p)^2} \tag{66}$$

with

$$\kappa = \frac{\tau}{\nu} \tag{67}$$

which we have called the kinetic ratio: the ratio of the mass-transfer kinetic constants in the flow direction and between the mobile phase and stationary phase.

For the third derivative:

$$F_r^{(3)} = 6\tau \frac{(r^2+2rs+s\nu)(r+r_1)(r+r_2) - (2r+\nu+\tau)(r^3+3r^2 s+3rs\nu+s\nu^2-\tau s^2+\tau s\nu)}{(r+r_1)^4(r+r_2)^4} \tag{68}$$

$$F_{r=0}^{(3)} = -6\frac{1+\kappa(2+\kappa)(1-p)}{(\tau p)^3} \tag{69}$$

The first moment about the origin is obtained by combining Eqs. (29) and (64). This yields Eq. (31), which indicates that there is no change in the peak location with respect to the equilibrium conditions. From Eqs. (33), (64) and (66), we obtain:

$$\mu_2' = \frac{N(N-1)}{(\tau p)^2} + 2N\frac{1+\kappa(1-p)}{(\tau p)^2} \tag{70}$$

and the variance for slow mass-transfer conditions (see Eq. (32)):

$$\mu_2 = \sigma^2 = \frac{N}{(\tau p)^2}[1+2\kappa(1-p)] = \frac{t_R^2}{N}[1+2\kappa(1-p)] \tag{71}$$

By combining Eqs. (38), (64), (66) and (69):

$$\mu_3' = \frac{N(N-1)(N-2)}{(\tau p)^3} + \frac{6N(N-1)}{(\tau p)^3}[1+\kappa(1-p)] + \frac{6N}{(\tau p)^3}[1+\kappa(2+\kappa)(1-p)] \tag{72}$$

From Eq. (37), the third moment is given by:

$$\mu_3 = \frac{2N}{(\tau p)^3}[1+3\kappa(1-p)(1+\kappa)] = \frac{2t_R^3}{N^2}[1+3\kappa(1-p)(1+\kappa)] \tag{73}$$

and the peak skewness is estimated from:

$$\gamma_1 = \frac{\mu_3}{\mu_2^{3/2}} = \frac{2}{N^{1/2}}\frac{[1+3\kappa(1-p)(1+\kappa)]}{[1+2\kappa(1-p)]^{3/2}} \tag{74}$$

Note that at equilibrium conditions, $\kappa = 0$ and Eqs. (71) and (74) give rise to Eqs. (36) and (42).

3. Experimental

The probe compounds were the diuretics xipamide (kindly donated by Lacer, Barcelona, Spain), benzthiazide and furosemide (Sigma, St. Louis, MO, USA). The drugs were dissolved in a few millilitres of acetonitrile, assisted by an ultrasonic bath and diluted with water. The concentration of the injected solutions was 10 μg/mL.

The chromatographic column was a Zorbax SB C18 (Agilent, Waldbronn, Germany, 150 mm × 4.6 mm I.D. and 5 μm particle size), protected with a similar C18 guard column (30 mm × 4.0 mm I.D. and 5 μm particle size). The mobile phases were prepared with acetonitrile (Scharlab, Barcelona) and water. The pH was buffered at 3 with 0.01 M citric acid (Panreac, Barcelona) and NaOH (Scharlab). The pH of the mobile phases was measured after the addition of the organic solvent, using an electrode calibrated with aqueous buffers.

Nanopure water (Barnstead, Sybron, Boston, MA, USA) was used throughout. Probe compound solutions and mobile phases were filtered through 0.45 μm Nylon membranes with a diameter of 17 mm (Cameo) and 47 mm (Magna), respectively (Osmonics, Herental, Belgium).

The HPLC system (Agilent, Series 1100) consisted of an isocratic pump, an automatic sampler, a UV-visible detector set at 254 nm, and a temperature controller module set at 25 °C. The flow rate was in the 0.25 to 2 mL/min range, and the injected volume was 5 μL. Data acquisition was carried out with an HPChemStation (Agilent). The mathematical treatment was implemented in Visual Basic 6.0 (Microsoft, Seattle, WA, USA).

4. Results and discussion

4.1. Simulation of solute migration

The peak profile described by Eqs. (31) and (71) was checked by comparison with the profile obtained by simulation of the solute migration, which is explained in this section. For this purpose, we assumed a hypothetical column divided in $N = 1000$ theoretical plates, with the total amount of solute in the mobile phase initially ($t = 0$) associated to the first theoretical plate.

The transference of the mobile phase volume from one theoretical plate to the next was divided in $M = 100$ steps. In each step, a hundredth of the volume associated to a theoretical plate was moved to the next plate, which displaced another hundredth of the volume. This, in turn, was transferred to the next plate. After each transfer, the mobile phase in each plate was homogenized. The process, which takes place during a time interval:

$$\delta t = \frac{t_0}{N \times M} \tag{75}$$

is illustrated in Fig. 1. After homogenization, solute mass transfer between the mobile phase and stationary phase can be described by the following differential equations for each theoretical plate:

$$\begin{aligned} a_i^{(1)} &= -ma_i + sb_i \\ b_i^{(1)} &= ma_i - sb_i \end{aligned} \tag{76}$$

whose solution yields:

$$a_i = a_{eq,i} + (a_{i,0} - a_{eq,i})e^{-\nu\delta t} \tag{77}$$

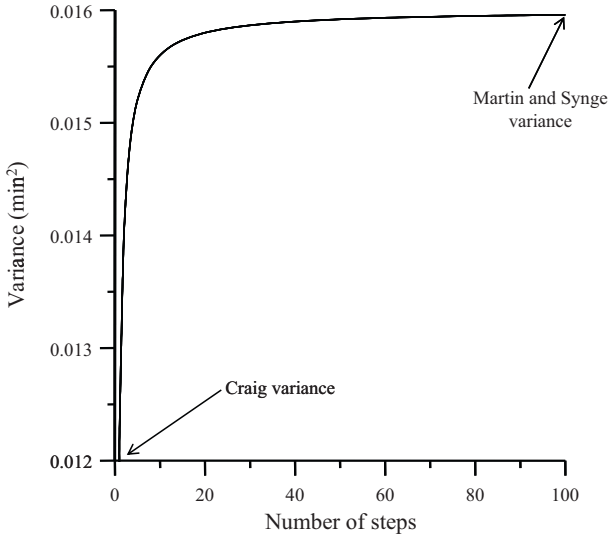

Fig. 2. Dependence of the peak variance with the number of steps (M), in the transference of a volume of mobile phase from one theoretical plate to the next one, corresponding to the simulation of solute migration. Parameters: $N = 1000$, $t_R = 4$ min, and $t_0 = 1$ min.

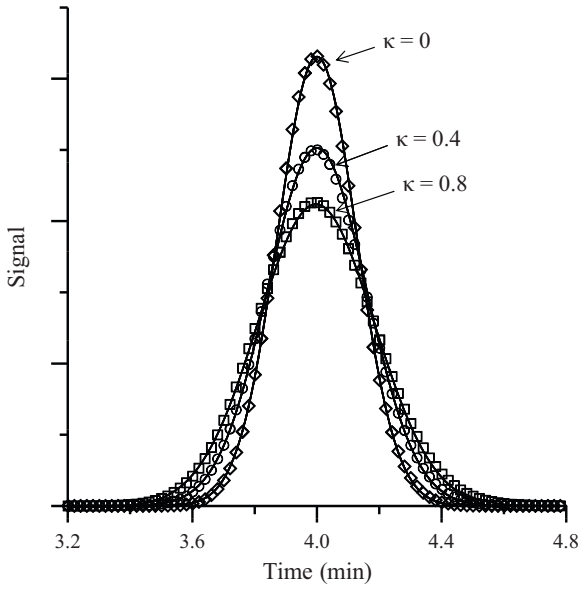

Fig. 3. Peaks depicted using the simulation approach (symbols) and Eq. (71), assuming a Gaussian behaviour (solid lines) for $N = 1000$, and different kinetic ratios (κ).

$$b_i = b_{eq,i} + (b_{i,0} - b_{eq,i})e^{-v\delta t} \quad (78)$$

where v is described by Eq. (43), δt takes the value given by Eq. (75), and:

$$a_{eq,i} = (a_{0,i} + b_{0,i})p \quad (79)$$

$$b_{eq,i} = (a_{0,i} + b_{0,i})(1 - p) \quad (80)$$

where p is defined by Eq. (9), and $a_{0,i}$ and $b_{0,i}$ are the initial concentrations of solute in the mobile phase and stationary phase, respectively, in the i theoretical plate at a given time (a multiple of δt). The process was repeated up to achieve full elution from the column in a summation of time intervals δt.

As observed in Eq. (75), the peak profile will depend on the assumed number of steps, M, in the transference of the mobile phase volume from one theoretical plate to the next one. Fig. 2 shows the change in the peak variance with M. The Craig approach assumes $M = 1$ (there is no additional broadening due to mixing of the portions of mobile phase inside a theoretical plate). The Martin and Synge approach is opposite: it considers a high M value. For further studies, the simulation was carried out for $M = 100$, which is sufficiently high to yield variance values close enough to those assumed in the Martin and Synge approach.

4.2. Agreement between the descriptions using the simulation approach and Eq. (71)

Fig. 3 depicts peaks simulated for an N value of 1000, assuming equilibrium conditions ($\kappa = 0$) and slow mass transfer for two values of the kinetic ratio (Eq. (67)): $\kappa = 0.4$ and 0.8. The peaks were drawn according to the simulation approach (symbols) and the predictions carried out with Eqs. (31) and (71) (solid lines). In the latter case, a Gaussian behaviour was assumed. As observed, the agreement between both approaches is highly satisfactory. The data show that as the kinetic ratio (κ) increases, the peak width is increased and the height, consequently, decreases. The simulated peaks show a small skewness, according to Eq. (74), with a ratio between the right and left half-widths at 10% peak height of 1.045, 1.051 and 1.063 for $\kappa = 0$, 0.4 and 0.8, respectively.

The variance values calculated with the simulation approach are compared in Fig. 4 with those predicted with Eq. (71) for hypothetical compounds exhibiting different retention times (p values). The high agreement between both approaches in different situations (i.e. different kinetic ratios and retention times) proves their validity. The linear dependence between the peak variance and the kinetic ratio (Eq. (71)) should be noted. The variance values at $\kappa = 0$ correspond to the equilibrium conditions. As the behaviour of the chromatographic column is moved away from equilibrium, κ increases, and consequently, the peak width, which is more apparent for the most retained compounds.

The term $2\,\kappa(1-p)$ in Eq. (71) is the increase degree of band broadening, expressed as peak variance due to the slow mass-transfer process.

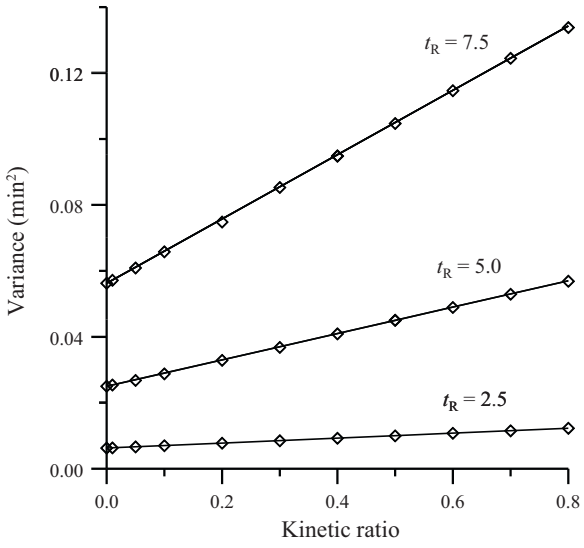

Fig. 4. Dependence of the peak variance on the deviation from the equilibrium conditions for three hypothetical compounds exhibiting different retention times (t_R, min) (p values from top to bottom: 0.133, 0.2 and 0.4, respectively). The points were obtained with the simulation approach and the lines correspond to Eq. (71). The efficiency was assumed to be $N = 1000$.

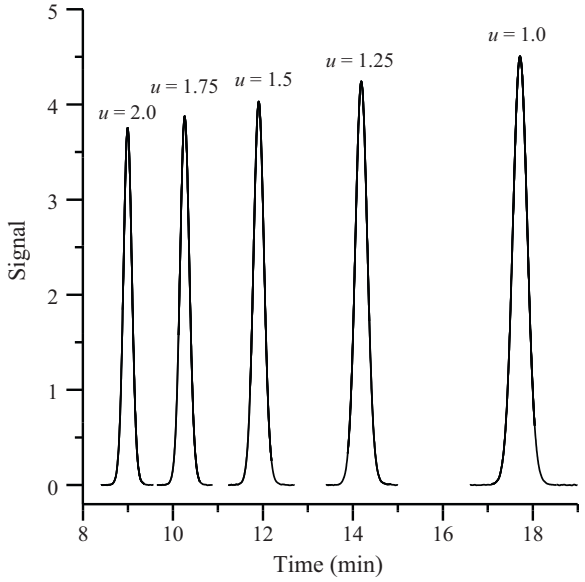

Fig. 5. Experimental elution profiles for xipamide in a Zorbax column, at different flow rates (u, mL/min).

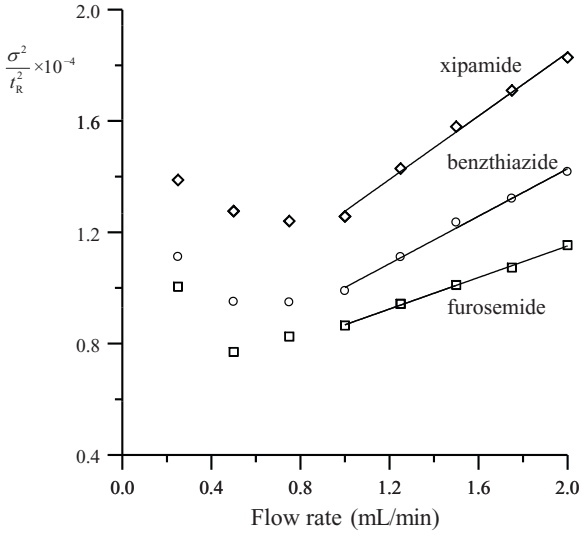

Fig. 6. van Deemter plots for the probe compounds.

4.3. Measurement of the deviations from the equilibrium conditions

The model developed in this work to predict the variance in slow mass-transfer conditions includes an additional parameter that relates the mass transfer in the flow direction (τ) with the mass transfer between the mobile phase and stationary phase (ν), the kinetic ratio (κ). This parameter measures the deviation degree from the equilibrium conditions, which depends on the mobile phase flow rate. At increasing flow rate, the time interval available to reach the equilibrium decreases. Consequently, the mass transfer between mobile phase and stationary phase will be moved away from the equilibrium.

We designed an experimental approach to evaluate the deviations from the equilibrium conditions in a chromatographic column (i.e. to obtain the mass-transfer kinetic ratio from experimental peaks). For this purpose, the kinetic ratio was expressed as:

$$\kappa = \frac{\tau}{\nu} = \frac{\tau_1}{\nu} u = \kappa_1 u \tag{81}$$

where τ_1 is the mass-transfer kinetic constant in the flow direction for a flow rate of 1 mL/min, and u is the flow rate. From Eqs. (71) and (81):

$$\frac{\sigma^2}{t_R^2} = \frac{1}{N} + 2\kappa_1 \frac{(1-p)}{N} u \tag{82}$$

The retention times and variances were obtained from the experimental data as the first moment about the origin, and the second moment about the mean, for the experimental elution profiles. For this purpose, the experimental peaks were numerically integrated using the Simpson's rule [25].

Fig. 5 depicts the experimental elution profiles for xipamide, eluted from a Zorbax column at several flow rates. Similar profiles were obtained for benzthiazide and furosemide, at their respective retention times. The reduction of the height at higher flow rate is due to the relative peak broadening. Fig. 6 illustrates the change in the σ^2/t_R^2 ratio for each compound. It can be seen that the behaviour is linear for $u > 1$ mL/min, where the contribution of diffusion is negligible. Eq. (82) describes this linear region. The slope of this line for a given compound will offer an estimation of κ_1. The column efficiency, N, can be obtained from the intercept of the line. However, this equation does not consider the extra-column broadening (σ_0^2), which will be only negligible for sufficiently retained compounds, and which changes with the flow rate. From Eqs. (9), (71) and (81):

$$\sigma^2 - \sigma_0^2 = \frac{t_R^2}{N}\left[1 + 2\kappa_1\left(1 - \frac{t_0}{t_R}\right)u\right] \tag{83}$$

where σ_0^2 was obtained at each flow-rate from the extrapolation to $t_R = 0$ of the σ^2 versus t_R^2 plot, using the data of the three probe compounds. Eq. (83) was non-linearly fitted using also all experimental (σ^2, σ_0^2, t_R, t_0, u) data obtained for the three probe compounds in the range 1–2 mL/min, in order to obtain the parameters N and κ_1. At 1 mL/min, the retention times for the probe compounds were 17.72, 10.27 and 6.54 min, and the column dead time was 1.19 min. The fitted parameters were $N = 17500$ and $\kappa_1 = 0.21$. Fig. 7 shows the good agreement between the experimental data and the predicted values according to Eq. (83).

For the case of study, $\sigma_0^2 = 0.0020\,\text{min}^2$ at a flow rate of 1 mL/min, which should be compared with the peak variance of each peak ($\sigma^2 = 0.0272$, 0.0104 and 0.0054 for xipamide, benzthiazide and furosemide, respectively). It should be noted that N in

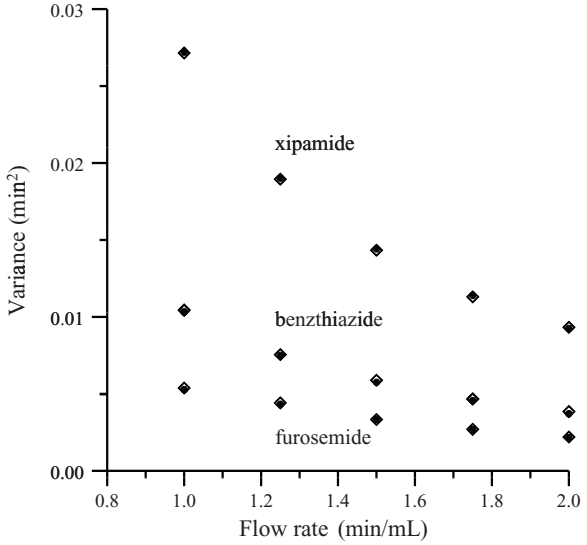

Fig. 7. Dependence of the peak variance on the flow rate for the probe compounds Experimental data (◊) and values predicted with Eq. (83) (●) are given.

Eq. (83) is the column efficiency at equilibrium conditions [26], which is the theoretically maximal efficiency that could be achieved at sufficiently rapid mass-transfer ($\nu = \infty$).

5. Conclusions

We have demonstrated that the Martin and Synge approach can be extended to describe slow mass-transfer conditions between the mobile phase and stationary phase. The proposed model predicts an additional peak broadening due to the slow mass transfer, which agrees with the van Deemter description when the solute diffusion is negligible. In contrast, the slow mass transfer does not yield any significant peak skewness. One of the known factors that produce the peak skewness typically observed in liquid chromatography is the behaviour described by non-linear isotherms, which makes solutes to migrate at different velocities along the column, depending on the mobile phase concentration.

The approach was validated by comparison with the simulation of solute migration through the theoretical plates, where the transference of the mobile phase volume from one theoretical plate to the next was assumed to occur in small steps, after which the mobile phase is homogenized. According to the proposed approach, the theoretical plate has a physical meaning: in a chromatographic column there are microscopic regions where a mixture is produced between the δV volume of mobile phase that reaches a given region and the existing volume of mobile phase in that region.

The measurement of the band broadening in experimental peaks at varying flow rate allows the evaluation of the kinetic ratio in the extended Martin and Synge model proposed in this work, which is a parameter related to the excess of band broadening due to the slow mass transfer. It should be noted, however, that the extended Martin and Synge model described in this work has the same practical limitations of the original model: it considers that the partition coefficient does not depend on the concentration, and that there is no interaction among solutes.

Acknowledgments

This work was supported by Project CTQ2010–16010/BQU (Ministerio de Ciencia e Innovación of Spain) and FEDER funds.

Appendix A.

To perform the transformation of Eq. (60) to the time-domain, the function must be decomposed in simple fractions as follows:

$$f_n(r) = \tau^N \left(\frac{r+s}{(r+r_1)(r+r_2)} \right)^N = \tau^N \sum_{i=1}^{N} \left(\frac{\beta_i}{(r+r_1)^i} + \frac{\delta_i}{(r+r_2)^i} \right) \quad \text{(A1)}$$

Assuming that, close to the equilibrium, the flow rate (expressed as the number of theoretical plates per time unit) is much smaller than the mass-transfer rate between both phases ($\tau \ll \nu$), then $r_2 \gg r_1$ (see Eqs. (56) and (57)), and the δ_i terms in Eq. (A1) will be sufficiently small to make:

$$f_n(r) \approx \tau^N \sum_{i=1}^{N} \frac{\beta_i}{(r+r_1)^i} \quad \text{(A2)}$$

The β_i coefficients can be calculated by applying the Heaviside's cover-up method [27]:

$$\beta_{N-j} = \frac{1}{j!} \left[\frac{d^j G(r)}{dr^j} \right]_{r=-r_1} = \frac{G^{(j)}(r)_{r=-r_1}}{j!} \quad \text{(A3)}$$

where from Eq. (A1):

$$G(r) = f_n(r)(r+r_1)^N = \left(\tau \frac{r+s}{r+r_2} \right)^N \quad \text{(A4)}$$

The first and second derivatives of Eq. (A4) are:

$$G^{(1)}(r)_{r=-r_1} = N\alpha^{N-1} \frac{\tau - \alpha}{R} \quad \text{(A5)}$$

$$G^{(2)}(r)_{r=-r_1} = N(N-1)\alpha^{N-2} \frac{(\tau-\alpha)^2}{R^2} - 2N\alpha^{N-1} \frac{\tau-\alpha}{R^2} = N(N-1)\alpha^{N-2} \frac{(\tau-\alpha)^2}{R^2} \times \left(1 - \frac{2\alpha}{(N-1)(1-\alpha)} \right) \quad \text{(A6)}$$

where

$$\alpha = \frac{\tau(s-r_1)}{R} \quad \text{(A7)}$$

and from Eqs. (56) and (57):

$$R = \sqrt{(\nu+\tau)^2 - 4\tau s} = r_2 - r_1 \quad \text{(A8)}$$

Also, since $N \gg 1$ and $r_2 \gg r_1$, $R \approx r_2$:

$$G^{(2)}(r)_{r=-r_1} \approx N(N-1)\alpha^{N-2} \left(\frac{\tau-\alpha}{R} \right)^2 \approx N(N-1)\alpha^{N-2} \left(\frac{\tau-\alpha}{r_2} \right)^2 \quad \text{(A9)}$$

The same holds for higher order derivatives:

$$G^{(j)}(r)_{r=-r_1} = \frac{N!}{(N-j)!} \alpha^{N-j} \left(\frac{\tau-\alpha}{r_2} \right)^j \quad \text{(A10)}$$

By substituting Eq. (A10) in Eq. (A3):

$$\beta_{N-j} = \frac{N!}{j!(N-j)!} \alpha^{N-j} \left(\frac{\tau-\alpha}{r_2} \right)^j \quad \text{(A11)}$$

Taking into account that $i = N - j$, and from Eqs. (A2) and (A11):

$$f_n(t) = \sum_{i=1}^{N} \frac{N!}{(N-i)!i!} \alpha^i \left(\frac{\tau-\alpha}{r_2} \right)^{N-i} \frac{1}{(r+r_1)^i} \quad \text{(A12)}$$

Finally, considering the inverse Laplace transform (see Eq. (24)):

$$f_n(t) = \sum_{i=1}^{N} \frac{N!}{(N-i)!i!} \alpha^i \left(\frac{\tau-\alpha}{r_2} \right)^{N-i} \frac{t^{i-1}}{(i-1)!} e^{-r_1 t} \quad \text{(A13)}$$

which can be conveniently rewritten as:

$$f_n(t) = \sum_{i=1}^{N} \frac{N!}{(N-i)!i!} w^i (1-w)^{N-i} r_1^i \frac{t^{i-1}}{(i-1)!} e^{-r_1 t} \quad \text{(A14)}$$

where:

$$w = \frac{\alpha}{r_1} \quad \text{(A15)}$$

The integration between zero and ∞ of Eq. (A14) should yield the unity, since it is a normalized function:

$$\sum_{i=1}^{N} \frac{N!}{(N-i)!i!} w^i (1-w)^{N-i} = (w + 1 - w)^N = 1 \quad \text{(A16)}$$

References

[1] J.C. Giddings, H. Eyring, J. Phys. Chem. 59 (1955) 416.
[2] A. Velayudhan, M.R. Ladish, Adv. Biochem. Eng. Biotechnol. 49 (1993) 123.
[3] J.C. Bellot, J.S. Condoret, J. Chromatogr. A 657 (1993) 305.
[4] A. Felinger, Data Analysis and Signal Processing in Chromatography, Data Handling in Science and Technology Series, Elsevier, Amsterdam, 1998.
[5] A. Felinger, G. Guiochon, Chromatographia 60 (2004) S175.

[6] G. Guiochon, A. Felinger, D.G. Shirazi, A.M. Katti, Fundamentals of Preparative and Nonlinear Chromatography, Academic Press, Elsevier, 2006.
[7] M. Netopilík, J. Chromatogr. 1133 (2006) 95.
[8] C.F. Poole, The Essence of Chromatography, Elsevier, Amsterdam, 2003.
[9] A.J.P. Martin, R.L.M. Synge, Biochem. J. 35 (1941) 1358.
[10] L.C. Craig, J. Biol. Chem. 155 (1944) 519.
[11] L. Lapidus, N.R. Amundson, J. Phys. Chem. 56 (1952) 984.
[12] J.J. van Deemter, F.J. Zuiderweg, A. Klinkenberg, Chem. Eng. Sci. 5 (1956) 271.
[13] E. Kucera, J. Chromatogr. 19 (1965) 237.
[14] P.J. Karol, Anal. Chem. 61 (1989) 1937.
[15] P.J. Karol, J. Chromatogr. A 550 (1991) 247.
[16] T. Fornstedt, G. Zhong, G. Guiochon, J. Chromatogr. A 741 (1996) 1.
[17] K. Miyabe, G. Guiochon, Anal. Chem. 72 (2000) 5162.
[18] F. Dondi, M. Remelli, J. Phys. Chem. 90 (1986) 1885.
[19] A. Felinger, A. Cavazzini, M. Remelli, F. Dondi, Anal. Chem. 71 (1999) 4472.
[20] M. Evans, N. Hastings, B. Peacock, Statistical Distributions, 3rd ed., Wiley, New York, 2000.
[21] P.P.G. Dyke, An Introduction to Laplace Transforms and Fourier Series, Springer Verlag, London, 2001.
[22] M.R. Spiegel, S. Lipschutz, J. Liu, Handbook of Formulas and Tables, 3rd ed., McGraw-Hill, New York, 2008.
[23] J.P. Foley, J.G. Dorsey, Anal. Chem. 55 (1983) 730.
[24] G. Gotmar, T. Fornstedt, G. Guiochon, J. Chromatogr. A 831 (1999) 17.
[25] J.F. Epperson, An Introduction to Numerical Methods and Analysis, Wiley, New Jersey, 2007.
[26] J.J. Baeza-Baeza, S. Pous-Torres, J.R. Torres-Lapasió, M.C. García-Álvarez-Coque, J. Chromatogr. A 1217 (2010) 2147.
[27] Y.K. Man, Int. J. Math. Edu. Sci. Technol. 38 (2007) 247.